Petroleum Research 8 (2023) 439–454

Contents lists available at ScienceDirect

Petroleum Research

journal homepage: http://www.keaipublishing.com/en/journals/petroleum-research/

Full Length Article

Uncertainty quantification in the Permian Basin using conventional and modified bootstrap methodology

Chukwuemeka O. Okoli [a, b], Scott D. Goddard [c], Obadare O. Awoleke [a, *]

[a] Department of Petroleum Engineering, University of Alaska Fairbanks, Fairbanks, 99775, Alaska, USA
[b] National Energy Technology Laboratory, 1450 Queen Avenue SW, Albany, 97321, Oregon, USA
[c] Department of Mathematics & Statistics, University of Alaska Fairbanks, Fairbanks, 99775, Alaska, USA

ARTICLE INFO

Article history:
Received 28 January 2023
Received in revised form
8 June 2023
Accepted 8 June 2023
Available online 21 June 2023

Keywords:
Uncertainty quantification
Machine learning
Bootstrapping
Reservoir forecasting
Frequentist probabilistic models

ABSTRACT

Various uncertainty quantification methodologies are presented using a combination of several deterministic decline curve analysis models and two bootstrapping algorithms. These probabilistic models are applied to 126 sample wells from the Permian basin. Results are presented for 12–72 months of production hindcast given an average well production history of 103 months. Based on the coverage rate and the forecast error (with the coverage rate being more significant in our choice of the best probabilistic models) and using up to one-half of the available production history for a group of sample wells from the Permian Basin, we find that the CBM-SEPD combination is the best probabilistic model for the Central Basin Platform, the MBM-Arps combination is the best probabilistic model for the Delaware Basin, the CBM-Arps is the best probabilistic model for the Midland Basin, and the best probabilistic model for the overall Permian Basin is the CBM-Arps when early time data is used as hindcast and CBM-SEPD for when one-quarter to one-half of the data is used as hindcast. When three-quarters or more of the available production history is used for analysis, the MBM-SEPD probabilistic model is the best combination in terms of both coverage rate and forecast error for all the sub-basins in the Permian. The novelty of this work lies in its extension of bootstrapping methods to other decline curve analysis models. This work also offers the engineer guidance on the best choice of probabilistic model whilst attempting to forecast production from the Permian Basin.

1. Introduction

The challenge of forecasting production from hydrocarbon wells is not a new one. Some approaches engineers have used to address this challenge in past literature include using empirical, and mechanistic (analytical/semi-analytical and the numerical) methods. The discussion below summarizes recent literature on the subject matter.

Ogunyomi et al. (2014) applied a new approach using statistical and model-based analysis of production data to model production decline in hydraulically fractured horizontal oil wells. They obtained a realistic estimate of estimated ultimate recovery (EUR) by identifying the flow regimes and understanding the overall decline behavior. Khanal et al. (2015) forecasted EUR based on limited production data in light rich shale (LRS) gas condensate reservoirs using empirical decline curve analysis, physics-based reservoir simulation and statistical analysis. Their analysis provided insight into the long-term production behavior in LRS gas condensate reservoirs. Klie (2015) proposed the combination of analytical growth models and data-driven models to develop highly predictive surrogate models effective in moderate to long term forecast for steam-assisted gravity drainage (SAGD) operations in oil sands and reserves estimation in unconventional resources.

Makinde and Lee (2016a) presented the results of a study to determine whether simple decline models can be used to forecast production and estimate reserves of both oil and gas in shale volatile oil reservoirs. They tested a variety of hybrid and simple decline curve analysis (DCA) models on simulated and field data to determine which model was effective in forecasting in the boundary dominated flow regime. Their results show that the Arps decline curve model was efficient for forecasting in the boundary-dominated flow (BDF) regime and the Duong model and its hybrid

* Corresponding author.
E-mail address: ooawoleke@alaska.edu (O.O. Awoleke).

https://doi.org/10.1016/j.ptlrs.2023.06.001

alternatives overestimate production in shale volatile oil reservoirs and that overestimation increases with shorter production histories. They suggested a proposed Modified Duong model to help alleviate the problem of serious overestimate of future production by the Duong model. Makinde and Lee (2016b) applied a new data-driven semi-analytical and statistical technique with a combination of compositional reservoir simulation and the decline curve analysis method to reliably forecast production with a reasonable level of certainty.

Li and Han (2017) developed a machine learning approach for forecasting conventional and unconventional reservoirs using reservoir properties and hydraulic fracture parameters as impute to the machine learning models. They applied a statistical approach using the neural network algorithm for production forecasting of single wells. Gorditsa et al. (2020) modeled the well performance of unconventional reservoirs using a high precision reservoir simulation model validated against analytical models and tested with numerous synthetic field cases. They established the most appropriate models for which to history match actual field cases using DCA models correlated against reservoir simulation results. Even though these empirical models are not based on physics, they are considered in practice to be consistent with the physics of hydrocarbon production. This is because these models have been validated with many field observations (Liu et al., 2021).

All the above researchers have focused on choosing the best deterministic or combination of deterministic models for any particular production dataset/history. This is somewhat related to quantifying the epistemic uncertainty. Our focus in this paper is to attempt to quantify the random or aleatory uncertainty associated with probabilistic decline curve analysis.

Jochen and Spivey (1996) were the first to apply the conventional bootstrap method to two water-flooded oilfields. They generated 1000 synthetic datasets from the actual production data and then utilized nonlinear regression to acquire estimates of the decline curve parameters for each synthetic dataset. Subsequently, parameter estimates obtained from the synthetic datasets were then used to forecast reservoir performance and approximate the distribution of reserves estimate. The main advantage of the conventional bootstrap over other decline curve analysis methods is that it does not require the analyst to have prior information about the probability distribution of parameters used in the decline curve analysis.

However, since production data is a sequence of observation that is time-dependent, Cheng et al. (2010) developed the modified bootstrap approach to correct for the underestimation of uncertainty that results from the conventional bootstrap method. They called this approach the “Modified Bootstrap Method with Block Re-sampling” to obtain reliable confidence intervals and improve the probabilistic estimates of oil and gas reservoirs. The modified bootstrap approach is more robust than the conventional bootstrap method. The result from Cheng et al.‘s application showed that the modified bootstrap methodology has a better coverage rate (83%) than the conventional bootstrap method (34%). This approach led to an accurate estimation of reserves and better prediction of P50 values than the conventional bootstrap approach (Cheng et al., 2010). However, their approach was tested using only the Arps equation. To the best of our knowledge, Cheng et al. (2010) did not comment on the difficulty of implementing the modified bootstrap method or how much computational effort it took to achieve their results. However, Purvis and Kuzma (2016) stated that the modified bootstrap method was time-intensive, challenging to implement, required wells to have no large abnormality in declines, and to be properly filtered. The works of Jochen and Spivey (1996) and Cheng et al. (2010) were based in the frequentist paradigm.

Gong et al. (2014) were the first to provide uncertainty bounds using the Arps' equation (Arps, 1945) and the Bayesian paradigm. Their proposed method reliably quantifies uncertainty in estimating reserves and requires the analyst to have prior information about the parameters used in the decline curve analysis (expressed as probability distribution). They used a Metropolis-Hastings algorithm for MCMC sampling to estimate the posterior distribution. Their Bayesian methodology was coupled with three DCA models based on Arps’ equation (Arps, Arps with 5% minimum decline, and modified Arps) and tested on 167 horizontal fractured Barnett shale gas wells. Their result shows that the probabilistic Bayesian method quantifies uncertainty with narrower P90 to P10 intervals, and computation time was faster than the modified bootstrap method. Their results indicate that, as the amount of available monthly production data for history-matching increases, uncertainty in production forecast decreases.

Building on the work of Gong et al., Paryani et al. (2017) introduced an Approximate Bayesian Computation method with rejection sampling to quantify the uncertainty associated with the decline curve analysis model by incorporating the models with an approximate Bayesian probabilistic methodology. The method simplified the Bayesian inference by approximating the complex likelihood function. In Approximate Bayesian Computation (ABC), a large number of simulated (or synthetic) production datasets were generated by using different values of the parameters of the decline curve equation in the Arps’ model. Based on an optimal threshold value, the synthetic datasets and their generating parameters are either accepted or rejected, and then the posterior could be approximated from the accepted parameters. Paryani et al. (2017) tested the techniques on 100 gas wells and 21 oil wells. They observed that when the approximate Bayesian computation was coupled with rejection sampling, the methodology reliably quantifies uncertainty in shale reservoirs, and the estimates from the ABC methodology were well-calibrated.

Korde et al. (2021) extended the work of both Gong et al. (2014) and Paryani et al. (2017) in that they combined the Bayesian and Approximate Bayesian framework with decline curve models other than the Arps' equations. The Gibbs sampler, Approximate Bayesian Computation, and the Metropolis-Hastings (MH) algorithms were the three different sampling algorithms utilized to sample parameter values from their posterior. The DCA equations tested in this work are the Arps' model, Power Law Exponential (PLE) model, the Stretched Exponential Production Decline (SEPD) model, Duong's model, and the Logistic Growth Analysis (LGA) model. They tested the methodology using 74 oil and gas wells in the Permian Basin with as low as six months of production hindcast. Based on the data analyzed in this study, LGA is best in terms of prediction errors for all algorithms except MH. The Gibbs algorithm is nearly the best algorithm in terms of prediction error for all DCA models except Arps. Prediction errors are the highest in the Central Basin platform. They also found that the hindcast length is very influential in determining the prediction error, coverage rate, and interval width of a model's predictions. They finally concluded that fitting multiple probabilistic models to data is recommended for greater confidence in model predictions, especially if such predictions are in agreement.

There is some advantage to using multiple flow regimes in production data analysis (use of hybrid models), but their limitation is that we typically do not know when to apply the different models that make up the hybrid model. Diagnostic plots offer some help but can be subjective especially when used to model transition flow periods that can occur for a long time because there are generally no known models to fit this flow regime adequately. Kong et al. (2020) did model the transition flow period in their work, but they did so for only the Arps model. Based on the foregoing, we have ignored the use of flow regime analysis in this work and

focused on quantifying the general uncertainty ascribed to the different decline curve models. Incorporating the use of hybrid flow models for the other decline curve models would be the subject of future work.

In this paper, we focus on the frequentist paradigm and will further expand the work of Jochen and Spivey (1996) and Cheng et al. (2010) by extending the conventional and modified bootstrapping algorithms to other DCA models other than the Arps' equation. The other DCA models considered in this work (in addition to Arps) are the Duong, and the SEPD models. The probabilistic framework was applied to 126 hydraulically fractured oil wells from the Permian Basin. We will not discuss the geology of the Permian Basin here. We refer the reader to Ward et al. (1986) and U.S. EIA (2020).

Based on the above, the objectives of this paper are as follows: (1) To apply the Conventional Bootstrap and Modified Bootstrap with Block resampling methodology to the Arps' hyperbolic decline curve model, the Duong's model, and the Stretched Exponential decline curve model in the **R** programming environment (R Core Team 2022); (2) to develop pseudocodes that will help the reader be able to reproduce the results we discuss here; (3) to determine if uncertainty in production forecasts can be reliably quantified using bootstrapping and the Duong's/SEPD models in a computationally manageable manner; (4) to determine which combination of DCA model and bootstrapping algorithm gives the best probabilistic forecast and coverage rates in the Permian Basin as a function of the production history used in the analysis.

2. Methods

The goal of this section is to present the methodologies applied in this paper. Two probabilistic approaches, namely the conventional bootstrap and the modified bootstrap with block resampling approach, are applied with the Arps (1945), Duong's (Duong, 2011), and SEPD (Valko and Lee, 2010) decline curve analysis models. The computational algorithms for both the conventional and modified bootstrap are also presented. The bootstrap is a class of methods involving the repeated resampling of observed data in order to approximate the sampling distribution of the parameter estimates in a model. With respect to reserves estimation, bootstrap methods are useful for making probabilistic forecasts of production without the need to have “prior” knowledge of the parameters' likely values. The conventional bootstrap assumes that production data are independent and identically distributed, which can be a weak point for it. Typically, pro-duction data are not independent and identically distributed but a sequence of observations occurring in chronological succession (i.e., a time series) with a generally declining trend (Cheng et al., 2010). For time series data with autocorrelation and a general variance structure, Cheng et al. (2010) proposed a more robust model-based modified approach to the bootstrap to preserve the structure of the original time series data using blocks. This approach was called “modified bootstrap with block resampling.”

2.1. Production data collection and cleaning

We tested the methodology of this research using production data obtained from publicly available and downloadable oil and gas production data. This data was made available by the Railroad Commission of Texas (or Texas Railroad Commission, RRC) and production data from the data analytics firm, Enverus (formerly known as Drillinginfo). We selected unconventional reservoirs in the Permian basin as a case study due to the vast potentials of the basin and its importance to the U.S. oil and gas industry. The wells selected for this case study were 126 unconventional wells. The wells were within the three main sub-basins of the Permian basin, namely, Central Basin Platform, Delaware Basin, and Midland Basin. Table 1 shows the number of oil wells analyzed from three sub-basins in the Permian Basin.

Active oil wells produced by horizontal drilling technology and completed within the last decade from 2010 to 2020 were selected. We filtered the wells by removing oil wells producing with a maximum producing rate of less than 5 bbls/day of oil. If an oil well has a maximum producing rate of less than 5 bbls/day, it would be considered a low-producing well. In some cases, such wells may be shut down or abandoned if they are no longer economically viable to operate. The choice of 5 bbls/day as a limiting threshold may be somewhat arbitrary but reflects an understanding that a well producing at such low rates is not a healthy well. The goal of this filtering process was to obtain well data that generally depicts a decline. We set the minimum production history for each well at 90 months or seven and a half years, with the most prolonged production period without stimulation used as a criterion for selecting the data. This means for a well that has undergone some stimulation in the last decade, the interval between the initial production date to date of stimulation or from the first production date after re-stimulation was used as production data for the case study. The production data length threshold was chosen to ensure that we have an adequate number of wells with a statistically significant number of data points in each well's production history. In summary, the wells used in this case study were selected based on the following criteria:

(1) Wells should have similar completion strategy and should be located in geographically similar areas,
(2) Wells should have a minimum of 90 months of production activity,
(3) Wells with no decline or wells with extreme spikes in production data were excluded,
(4) Production data with no trend were excluded.

2.2. Summary of DCA models

We applied the Arps' model, Duong's model, and the Stretched Exponential model in the methodology part of this paper. Other decline curve models, such as the Power Law Exponential and Logistic Growth model, are not discussed in this work due to time constraints and will be part of a future investigation.

2.2.1. Arps' decline curve model

The Arps' **hyperbolic** decline curve equation is given as:

$$q(t) = \frac{q_i}{(1 + D_i b t)^{\frac{1}{b}}} \tag{1}$$

where: q is the current production rate, q_i is the production rate at time zero, b is hyperbolic decline constant, t is the time since the start of production, D_i is the initial nominal decline rate. For hyperbolic decline, the b value is between 0 and 1. When b equals 0, the decline is exponential, and when b equals 1, the decline is

Table 1
Unconventional Permian Basin wells used in the case study.

Basin	Sub Basin	No. Of Wells	Production Type
Permian Basin	Central Basin Platform	42	Oil
	Delaware Basin	35	Oil
	Midland Basin	49	Oil

harmonic.

For Arps' **exponential** decline, the decline curve equation is given as:

$$q(t) = q_i \exp(-D_i t) \tag{2}$$

For Arps' **harmonic** decline, the decline curve equation is given as:

$$q(t) = \frac{q_i}{(1 + D_i t)} \tag{3}$$

2.2.2. Duong's model

Duong (2011) developed a model to estimate the ultimate recovery for wells with fracture dominated flow and negligible matrix contribution. He tested field data from several shale gas plays and plotted log-log plots for rate over cumulative production versus time in

days giving a straight line with a negative slope, $-\ m$, and an intercept a such that:

$$\frac{q}{G_p} = at^{-m} \tag{4}$$

From the expression for the slope, m is positive and greater than 1 for shale reservoirs. An m value less than 1 could signify a conventional tight well. Duong (2011) derived an expression for the gas flow rate q and cumulative production G_p as follows:

$$q = q_i t^{-m} \exp\left[\frac{a}{1-m}\left(t^{1-m} - 1\right)\right] \tag{5}$$

$$G_p = \frac{q_i}{a} \exp\left[\frac{a}{1-m}\left(t^{1-m} - 1\right)\right] \tag{6}$$

where: q is the gas flow rate, G_p is cumulative production, a and m are constants for a given dataset derived from the log-log plot of q/G_p versus time in days, q_i is the rate at day 1, t is production time.

Duong (2011) determined four parameters (a, m, q_i, q_∞) for the model using two stages of sequential ordinary least square regression. By taking the log of both sides in Eq. (4), parameters a and m were obtained by least square regression from the intercept and slope of:

$$\log\left(\frac{q}{G_p}\right) = -m \log(t) + \log a \tag{7}$$

To determine q_i, the gas flow rate q is plotted against $t(a, m)$ and a linear model is fit without an intercept whose slope determines q_i. However, due to conditions in the wellbore, an intercept can be necessary in some cases. This means that the production at infinite time q_∞ is not zero. To obtain a solution for q_i and q_∞, another sequence of ordinary least square regression was done:

$$q = q_i t(a, m) + q_\infty \tag{8}$$

where:

$$t(a, m) = t^{-m} \exp\left[\frac{a}{1-m}\left(t^{1-m} - 1\right)\right] \tag{9}$$

Duong et al.'s model is advantageous due to its numerical stability when fitting the curve. Also, the solution obtained is unique.

2.2.3. Stretched-exponential model

Valko and Lee (2010) proposed the Stretched-Exponential model to be applied for a quick evaluation of datasets of rate behaviors. In formulating the model, they assumed that the rate behavior agrees with the stretched exponential decay and is of the form:

$$q = \hat{q}_i \exp\left[-\left(\frac{t}{\tau}\right)^n\right] \tag{10}$$

where: $\hat{q}_i$ is rate "intercept," n is time "exponent," and τ is the characteristic time constant. To obtain n and τ parameters, Valko and Lee (2010) estimated one-third, two-third, and the last point of cumulative production, i.e., given three years of production history, cumulative production is calculated at year-end. The ratio of the second year to the first year cumulative (ratio of two-third to one-third) and the third year to the first year cumulative (ratio of last point to one-third) are calculated using the equation below.

$$r_{21} = \frac{Q_{second\ year}}{Q_{first\ year}}, r_{31} = \frac{Q_{third\ year}}{Q_{first\ year}} \tag{11}$$

Solving the two nonlinear equations shown by the expression below, the n and τ parameters can be calculated:

$$\frac{\Gamma\left[\frac{1}{n}\right] - \Gamma\left[\frac{1}{n}, \left(\frac{24}{\tau}\right)^n\right]}{\Gamma\left[\frac{1}{n}\right] - \Gamma\left[\frac{1}{n}, \left(\frac{12}{\tau}\right)^n\right]} = r_{21} \tag{12}$$

$$\frac{\Gamma\left[\frac{1}{n}\right] - \Gamma\left[\frac{1}{n}, \left(\frac{36}{\tau}\right)^n\right]}{\Gamma\left[\frac{1}{n}\right] - \Gamma\left[\frac{1}{n}, \left(\frac{12}{\tau}\right)^n\right]} = r_{31} \tag{13}$$

where $\Gamma(t)$ and $\Gamma(s, x)$ are the gamma function and the incomplete gamma function, respectively, given as:

$$\Gamma(t) = \int_0^\infty x^{t-1} e^{-x} dx \tag{14}$$

$$\Gamma(s, x) = \int_x^\infty t^{s-1} e^{-t} dt \tag{15}$$

Can and Kabir (2011) concluded that the stretched-exponential decline model (SEPD) is better than the Arps' hyperbolic equation for estimating reserves of unconventional wells primarily due to the bounded nature and linear behavior of the expression for recovery factor.

2.3. Summary of probabilistic approach

2.3.1. Conventional bootstrap approach

To carry out the conventional bootstrap approach, we resample data with replacement. There are two major assumptions made in using the bootstrap method for probabilistic reserve estimation. Firstly, the production dataset available is assumed to be independent and identically distributed. The second assumption is that there is a decline curve model available to predict reservoir performance.

The manner of generating a probability forecast from the decline curve model is through "hindcasting," where a fraction of the known data is entered in the model, and the output is validated by comparison with the actual data. The bootstrap process begins by generating a large number of bootstrap samples from the "hindcast" of the original production dataset by randomly sampling points from the "hindcast" dataset with replacement. The bootstrap samples obtained are the same size as the original hindcast dataset. After that, regression techniques (either linear or nonlinear) are

used to fit a deterministic model to the bootstrap sample and thereby estimate the parameters of the decline curve model. The estimated parameters from the synthetic datasets are then plugged into the same model to produce predictions of future production. These predictions are then summarized to yield probabilistic reserves estimates.

2.3.2. Conventional bootstrap methodology

The overall workflow for the conventional bootstrap methodology using an arbitrary decline curve model is illustrated below:

(1) Set aside an initial fraction of the dataset as the hindcast and reserve the rest of the dataset to measure the prediction error between predicted and actual production.
(2) From the initial "hindcasted" production dataset, generate multiple bootstrap samples by randomly sampling with replacement. Each bootstrap realization has the same size as the hindcast.
(3) Estimate the parameters in the decline curve model by fitting the selected decline curve analysis model to the bootstrapped data using regression analysis.
(4) Using the estimated parameters and the decline curve analysis model, forecast production performance.
(5) Repeat steps 1 to 4, iterating through all the bootstrap samples.
(6) Summarize the overall distribution of reserves estimates by computing the (pointwise) 10th, 50th, and 90th percentiles of the reserves distribution.

2.3.3. Computational algorithms for conventional bootstrap method

In this section, we will illustrate the algorithm for uncertainty quantification using the conventional bootstrap with application to the Arps', SEPD, and Duong's decline curve models. For ease of computing, we use the **R** programming environment for computation and analysis. The conventional bootstrap method begins by generating a large number of bootstrap datasets of production by random sampling with replacement from the hindcast of the original production dataset. That is, for a set of m_1 data points, multiple bootstrap samples are obtained by sampling randomly with replacement n times (each of size m_1) from the hindcast dataset. This means that after sampling a particular data point, it is "replaced" back in the original dataset, and it can be resampled again. Each bootstrap sample is fit using regression analysis to determine the decline curve parameters. In the case where the Arps' decline curve model is applied with conventional bootstrap methodology, nonlinear regression is applied to determine the decline curve parameters q_i, b, and D_i.

To do this, we first use a Taylor series approximation to linearize the Arps' model in order to estimate good starting parameters for the nonlinear fitting process (see Appendix A). A self-start function in R can also generate starting parameters for the nonlinear regression. Using the starting parameters, we obtained from the linearization process, nonlinear regression is done to determine the estimates of the parameters in the decline curve model. All the above steps are important to automate the non-linear regression process. We extrapolated the parameters obtained from the nonlinear fitting process to estimate future production. In addition to providing estimates of future production and reserves, the nonlinear regression also provides useful information about the sampling distribution of the estimates of the decline curve parameters q_i, b, and D_i and the uncertainty in reserves estimates. We measure this uncertainty with the confidence limits on the forecasted reserves, denoted as P90, P50, and P10.

The conventional bootstrap method with the Duong's decline curve model begins just like above by generating bootstrap samples of the hindcast dataset. Each bootstrap sample is fit using two stages of sequential ordinary least square (OLS) to obtain the four parameters a, m, q_i, and q_∞ of the Duong model. A flowchart describing the methodology is shown in Fig. 1. Firstly, the log of both sides in Eq. (4) is taken, and first stage sequential OLS regression to get parameters a and m from the bootstrap sample is done. Parameters a and m obtained from the regression are used to compute the time function $t(a, m)$ given by Eq. (9), and the second sequence of ordinary least square regression is carried out to obtain a solution for q_i and q_∞ in Eq. (8). The four parameters (a, m, q_i, q_∞) obtained from the two-stage sequential linear regression fitting process is extrapolated to estimate future production and reserves. Uncertainty in probabilistic estimates is obtained as P90, P50, and P10 values. This linear method of fitting production data using Duong's model is quite advantageous and faster than the Arps' model because the four parameters obtained by regressing Eq. (7) and Eq. (8) is a unique solution and minimizes the mean squared error (MSE) in a global sense. This is usually not true for the nonlinear regressed Arps equation. A presentation of the sequential linear regression analysis process used to obtain the Duong's model decline curve parameters is shown in Appendix B.

In the conventional bootstrap with the SEPD model, similar to the Arps' and Duong's models, bootstrap realizations of the hindcast dataset are generated. Initial starting parameters are estimated using a function in **R** and used in the nonlinear regression algorithm to estimate the parameters of the SEPD model, namely τ, n, and $\widehat{q}_i$. The parameters obtained from the nonlinear regression of the dataset are extrapolated to estimate future production and reserve. A flowchart describing the methodology is shown in Fig. 2. The parameters from nonlinear regression of the dataset are also used to estimate future production, the distribution of reserves, and uncertainty in reserves estimates, i.e., P90, P50, and P10 values.

2.3.4. Modified bootstrap approach

In the conventional bootstrap methodology, the assumption that production data is independent and identically distributed was made. However, production data is not independent and identically distributed but a sequence of observations occurring in succession (i.e., a time series) with an overall decline trend. For time series data with autocorrelation and general variance structure, Cheng et al. (2010) proposed a more robust modified approach to the bootstrap to preserve some of the original time series data structure within blocks. This approach was called the "modified bootstrap method with block resampling."

In the modified bootstrap approach, the production data $y_1, \ldots, y_n$ are fit using the decline model, producing fitted values $\widehat{y_1}, \ldots, \widehat{y_n}$ and residuals $e_1, \ldots, e_n$. These chronological residuals are split into blocks of size d: $b_1 = \{e_1, \ldots, e_d\}, \ldots, b_{n/d} = \{e_{n-d+1}, \ldots, e_n\}$. The blocks $b_1, \ldots, b_{n/d}$ are then resampled with replacement as if the conventional bootstrap were being performed with them, yielding bootstrap blocks ${b_1}^* = \{{e_1}^*, \ldots, {e_d}^*\}, \ldots, {b_{n/d}}^*$. The resulting bootstrap blocks of residuals are recombined in any order and the residuals are added to the model's fitted values to generate a new proper bootstrap dataset (${y_1}^* = \widehat{y_1} + {e_1}^*, \ldots$). The decline curve model is now fit to the new bootstrap data ${y_1}^*, \ldots, {y_n}^*$ using regression techniques, either linear or nonlinear regression, to estimate the model's parameters. The estimated parameters from the bootstrap dataset are then used to estimate future production and reserves.

To use the modified bootstrap, the analyst must decide how many residuals to include in the blocks that will be resampled. The

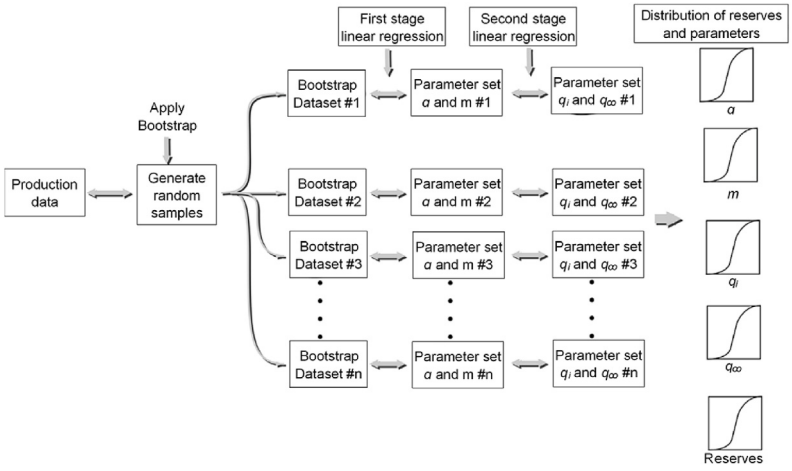

Fig. 1. Sequence for Conventional Bootstrap using Duong's model.

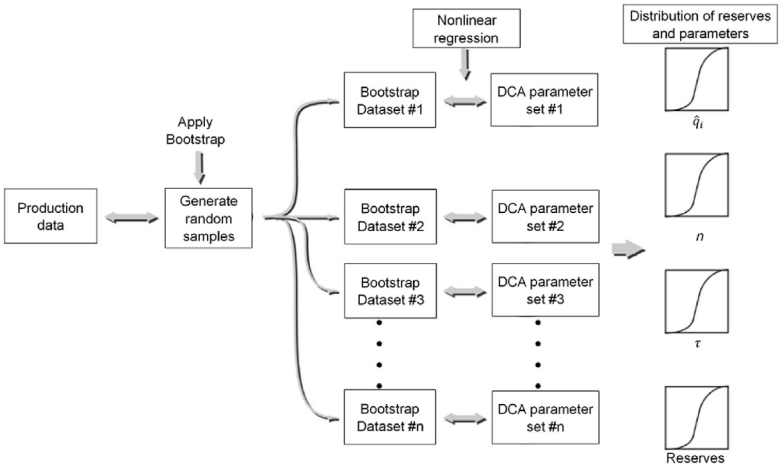

Fig. 2. Sequence for Conventional Bootstrap using SEPD model.

optimal block size in this paper was determined using an approach proposed by Cheng et al. (2010) which makes use of the residuals' autocorrelation function (acf). This function measures how observations in a time series are related to each other. For a sequence of data $y_1, y_2, \ldots, y_n$ at time $t_1, t_2, \ldots, t_n$, the sample autocorrelation function, r_k, at lag k is defined as:

$$r_k = \frac{\sum_{t=1}^{n-k}(y_t - \overline{y})(y_{t+k} - \overline{y})}{\sum_{t=1}^{n}(y_t - \overline{y})^2} \quad for\ k = 1, 2, \ldots \tag{16}$$

An example plot of r_k against lag time k is shown in Fig. 3. If the autocorrelation is high at some lag (the lag is a fixed amount of time between consecutive observations), i.e., the observations are strongly related to each other at some lag, it might be beneficial to capture some of this autocorrelation in the bootstrap samples. The proposal of Cheng et al. (2010) is that for a particular time series of residuals, the optimal block size will be the same as the lag distance k just before the autocorrelation function falls insignificantly close to zero—i.e. the maximal significant lag distance in the acf. In Fig. 3, the acf falls within a negligible distance of zero (as measured by the confidence bounds drawn as dashed lines) at a lag period of 8 months. Accordingly, the optimal block size for this case would be 7 months.

The algorithm to select the optimal block size is as follows:

(1) Calculate the confidence band.
(2) Calculate the autocorrelation function (acf).
(3) Using the autocorrelation function and confidence bands, determine the maximal lag time after which the autocorrelation does not significantly differ from zero.
(4) The lag time determined in step 3 is the optimal block size.

2.3.5. Modified bootstrap methodology

The overall workflow for the modified bootstrap methodology with an arbitrary decline curve model is described below:

(1) Set aside a fraction of the dataset as the hindcast and the rest of the dataset to estimate the misfit between predicted (forecast) and actual production.
(2) Fit the initial hindcast dataset with a decline curve model and compute residuals between the fitted model and observed data.

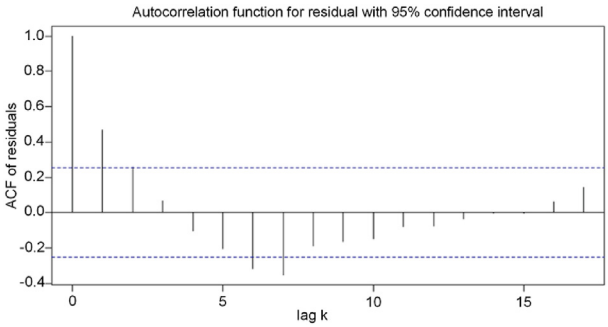

Fig. 3. Autocorrelation plot of residual for determining block size.

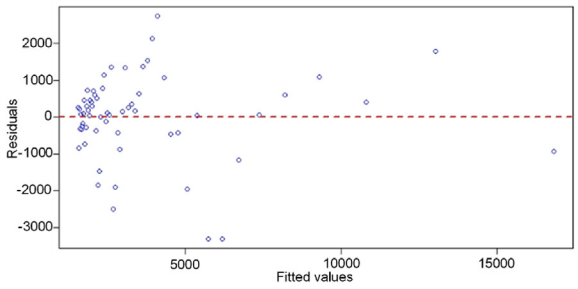

Fig. 4. A Plot of residuals versus fitted values.

(3) Determine the optimal block size using the autocorrelation function on the residuals and group the residuals into time intervals based on the optimal block size.
(4) Generate multiple block bootstrap samples of the residuals by randomly sampling blocks with replacement. Each bootstrap sample has the same size as the original hindcast.
(4) Add the block bootstrap samples of the residuals to the production fitted values to obtain bootstrap samples of production data.
(5) Compute the parameters in the decline curve model by fitting the selected decline curve analysis model to the bootstrap sample data using regression analysis.
(6) Using the fitted model, forecast production performance.
(7) Repeat steps 4 to 7, iterating until the last bootstrap sample.
(8) Summarize the distribution of reserves by computing the 10th, 50th, and 90th percentiles or forecasted production.

2.3.6. Computational algorithms for modified bootstrap method

In the modified bootstrap method, the hindcast is fit with nonlinear regression using the appropriate decline curve model. The residuals between the fitted data and actual production data are computed. A plot of residuals versus fitted data is shown in Fig. 4. As expected, there appears to be a certain amount of autocorrelation in these residuals. Accordingly, the residuals are grouped into time blocks based on the optimal block size, as described above. A plot of residuals as a function of time (with the optimal blocks shown) is depicted in Fig. 5. The block size is 7 months in this example.

Sampling with replacement is done on a block-by-block basis as opposed to sampling individual residual data points. The intent is to generate bootstrap samples of the hindcast fraction of the residuals. This approach is intuitive because correlation within the residuals is at least partially preserved as well as possibly other valuable structures in the data. Multiple block bootstrap samples of the residuals are obtained by random sampling with replacement. A flowchart describing the modified bootstrap methodology using Duong's DCA is shown in Fig. 6 and a flowchart describing the methodology as applied to the SEPD model is shown in Fig. 7.

3. Results and discussion

The case studies were carried out in order to:

(1) Generate probabilistic decline curve forecasts for production in sample unconventional hydraulically fractured horizontal wells in the Permian Basin,
(2) Calculate the forecast coverage rate, i.e., the percentage number of wells with actual cumulative production falling within the predicted P90 - P10 range for sample wells from the Permian basin,
(3) Compare actual cumulative production (P_{actual}) to forecasted P50 cumulative production and calculate prediction errors for a variety of hindcast fractions.

Hindcasting techniques were applied to quantify the uncertainty in the production forecast when applying the methodology. History matching was performed using only a portion of the production history, while the remaining portion was used for forecasting. The uncertainty in the forecast was measured by the forecast coverage rate. The mean absolute percentage error (MAPE) or average absolute error is the mean or average of the absolute percentage errors of forecasts. We defined the MAPE in this case as:

$$MAPE = Average* \frac{|P50 - P_{actual}|}{P_{actual}} \quad (17)$$

where P50 is reserves having a 50% certainty of being produced, and P_{actual} is actual or true value of reserves. The smaller the average absolute error, the better the forecast. In carrying out the analysis, the ideal scenario was for the MAPE to be at a minimum, and the forecast coverage rate for the P90 - P10 range be approximately 80% for a given hindcast fraction.

3.1. Choice of bootstrap sample size

To determine the number of bootstrap samples to use in this study, we ran a pilot case. It consists of applying the modified bootstrap methodology and the SEPD model to the rate data from 15 sample wells in the Permian Basin. We did a sensitivity analysis on the number of bootstrap samples, varying it from 10 to 10,000. We applied the preceding procedure for both the 12 and 48-month hindcast fractions. Table 2 and Table 3 shows the summary of results for bootstrap size selection determination at 12- and 48-months production hindcast data, respectively. The coverage rate, the cumulative P50 prediction, and error in the P50 prediction did not change appreciably as a function of the number of bootstrap samples for both 12 and 48 months. As expected, the 48-month results were better than those for the 12-month hindcast (53% vs. 33% for coverage rate and 10% vs. 38% for prediction error). Accordingly, in this paper, the bootstrap size used is 100.

3.2. Single well case study to illustrate the method

The methodology is illustrated using a single well drawn from

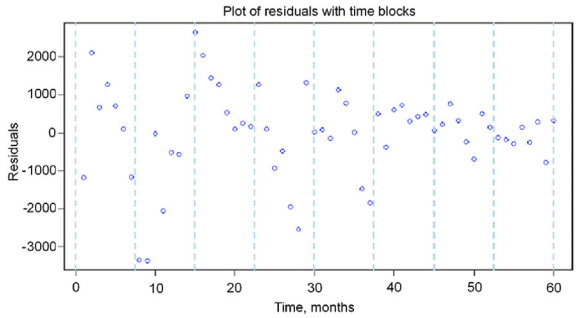

Fig. 5. A Plot of residuals with time blocks.

the Delaware Basin. In this study, we assumed that a portion of the production history is known and represented by 12, 24, 36, 48, 60, 72, and 84 months of production hindcast. The total amount of production history available is 120 months. The six scenarios that will be used to illustrate the methodology include:

(1) Conventional Bootstrap with Arps' model,
(2) Modified Bootstrap with Arps' model,
(3) Conventional Bootstrap with Duong's model,
(4) Modified Bootstrap with Duong's model,
(5) Conventional Bootstrap with Stretched Exponential model,
(6) Modified Bootstrap with Stretched Exponential model.

To illustrate the methodologies in the following sections, a 48-month hindcast will suffice unless otherwise specified.

3.2.1. Case 1: conventional bootstrap with Arps' model

We applied a given hindcast to generate 100 bootstrap samples. Using non-linear regression and the Arps' equation, 100 iterations of the Arps' decline curve parameter set, that is, q_i, b, and D_i, were generated. These parameter estimates were used to generate 100 predictions of future production. The P10, P50, and P90 estimates of both production rate and cumulative production as a function of time were generated.

Figs. 8 and 9 shows the plot of the production forecast and cumulative production, respectively, for 48 months of production hindcast. The actual production rate and cumulative production fall

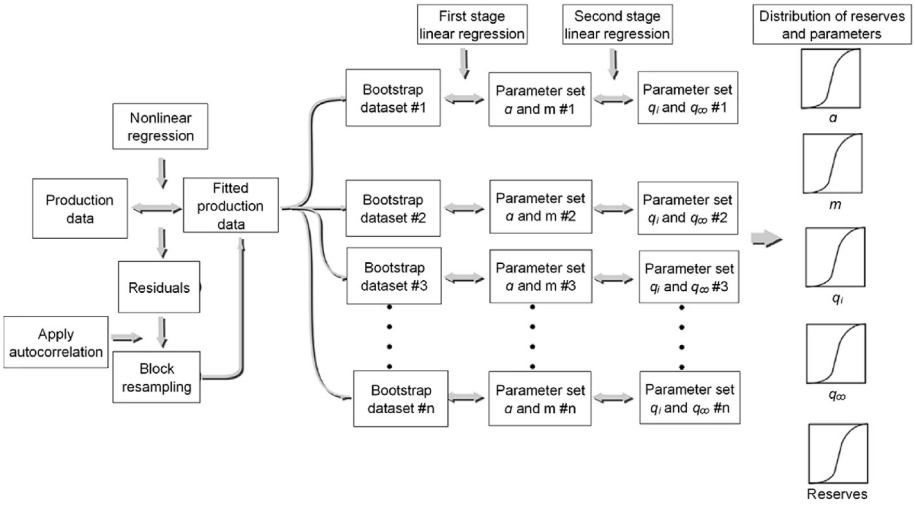

Fig. 6. Sequence for Modified Bootstrap using Duong's model.

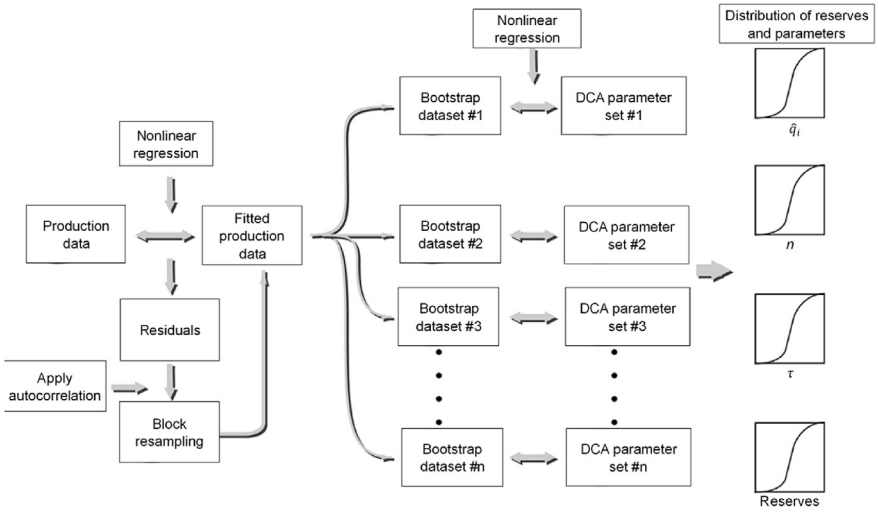

Fig. 7. Sequence for Modified Bootstrap using SEPD model.

Table 2
Performance of the modified bootstrap at 12 months of production hindcast, by bootstrap sample size.

Number of Bootstrap	10	50	100	200	500	1000	10000
Coverage Rate, CR (%)	26.67	33.33	33.33	33.33	33.33	33.33	33.33
Cumulative P50 Prediction, STB	1,842,452.01	1,801,567.97	1,823,647.48	1,864,795.89	1,867,125.22	1,857,656.61	1,854,708.81
Error in Cumulative P50 Prediction	39.94%	38.69%	38.15%	37.88%	37.89%	38.04%	37.88%

Table 3
Performance of the modified bootstrap at 48 months of production hindcast, by bootstrap sample size.

Number of Bootstrap	10	50	100	200	500	1000	10000
Coverage Rate, CR (%)	46.67	53.33	53.33	53.33	53.33	53.33	53.33
Cumulative P50 Prediction, STB	2,409,173.63	2,407,502.43	2,415,908.46	2,417,899.86	2,416,252.37	2,412,718.17	2,410,520.93
Error in Cumulative P50 Prediction	10.92%	10.45%	10.48%	10.41%	10.38%	10.52%	10.59%

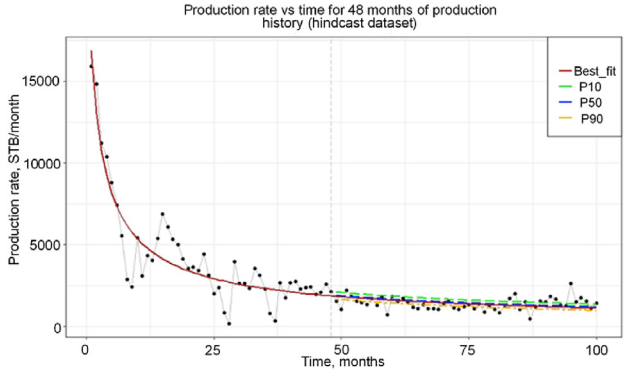

Fig. 8. The production forecast for 48 months of production data using Conventional Bootstrap with Arps' model.

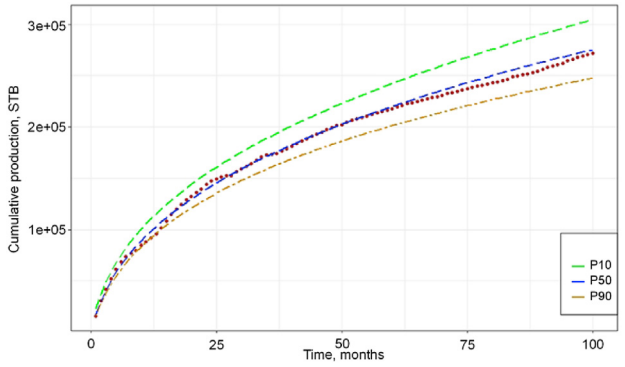

Fig. 9. Cumulative Production plot for 48 months of production data using Conventional Bootstrap with Arps' model ("red" dotted line is best fit line).

within the P90 - P10 range for the 48-month hindcast.

3.2.2. Case 2: modified bootstrap with Arps' model

First, we fit the hindcast dataset with the Arps model and then computed the residuals between the fitted model and observed data. A plot of residuals versus the fitted value for the 48-month hindcast is shown in Fig. 10. We utilized the autocorrelation function to determine the block size. The acf plot used to determine the block size for the 48-month hindcast dataset is presented in Fig. 11. With the optimal block size determined, we grouped the residuals into blocks. For the 48-month hindcast, the acf plot in Fig. 11 shows

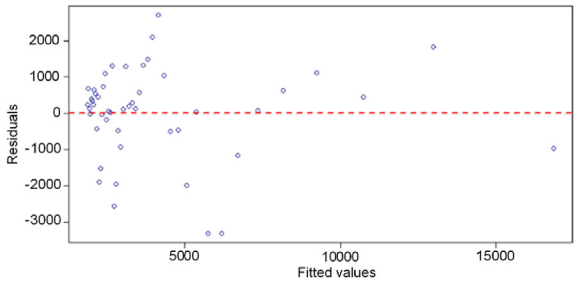

Fig. 10. Residual plot based on the model fit $\widehat{Y}_i$ of the Arps' equation for 48-months hindcast dataset.

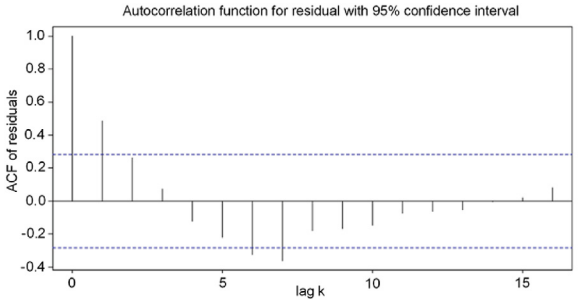

Fig. 11. Autocorrelation function for a single well case study at 48-month hindcast.

that the maximal lag value before which the acf value falls insignificantly close to zero is seven. This means the optimal block size for the 48-month hindcast is 7 months. The residuals are accordingly grouped into 7-month blocks, as seen in Fig. 12.

Multiple bootstrap samples are obtained by sampling blocks of residuals with replacement for the 48-month hindcast. We then obtain new bootstrap datasets by adding the bootstrap samples of residuals to the fitted production data. Parameters in the Arps' decline curve model are then estimated from the bootstrap data. Future production is then forecasted, and probabilistic reserves estimates can be determined. The production forecast plot for 48-month of production data is shown in Fig. 13. The plot also shows the probabilistic forecasts denoted as P90, P50, and P10 values.

Fig. 14 shows the cumulative production plot for 48 months of production hindcast. From Fig. 13, we observe that the actual production rate values fall mostly within the P90 - P10 range. Also, as seen in Fig. 14, the actual cumulative production is uniformly

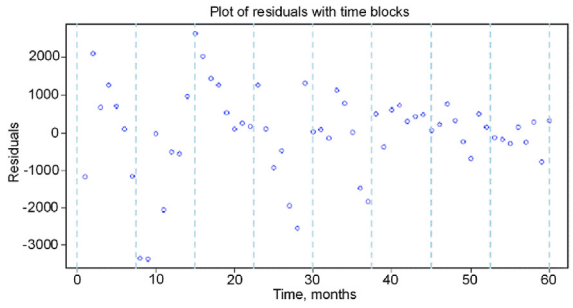

Fig. 12. Plot of Residuals with time blocks for 48-month hindcast of single well case study.

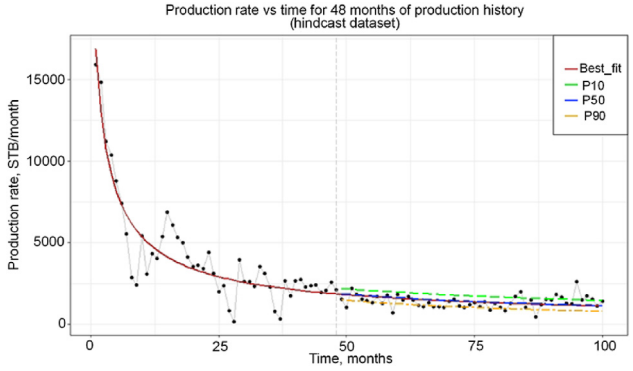

Fig. 13. The production forecast for 48 months of production data using Modified Bootstrap with Arps' model.

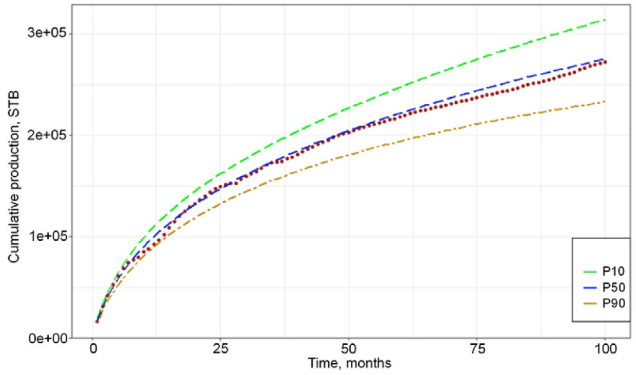

Fig. 14. Cumulative Production plot for 48 months of production data using Modified Bootstrap with Arps' model ("red" dotted line is best fit line).

within the P90 - P10 range.

3.2.3. Case 3: conventional bootstrap with Duong's decline curve model

For the application of conventional bootstrap methodology to the Duong's decline curve model, we used, as usual, a 48-month hindcast to generate multiple bootstrap samples. The parameters a, m, q_i, and q_∞ in Duong's model were obtained by applying the following two stages of sequential OLS regression.

Firstly, the logarithm of both sides in Eq. (4) was taken and OLS regression was performed to get parameters a and m from the

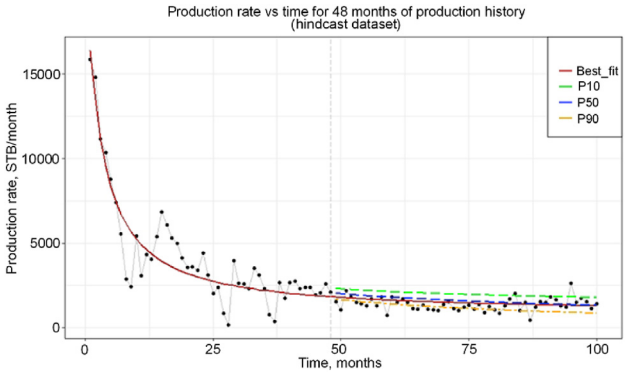

Fig. 15. The production forecast for 48 months of production data using Conventional Bootstrap with Duong's model.

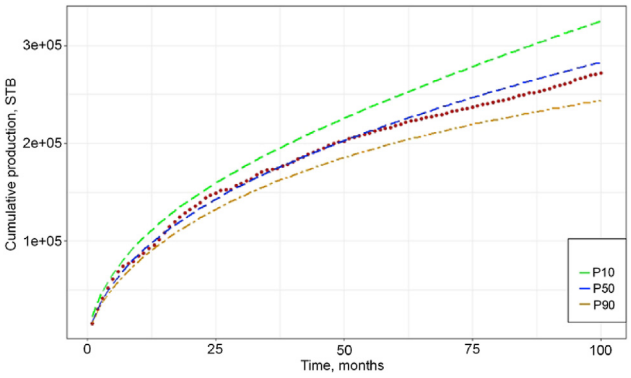

Fig. 16. Cumulative Production plot for 48 months of production data using Conventional Bootstrap with Duong's model ("red" dotted line is best fit line).

bootstrap dataset. Parameters a and m obtained from the regression were used to compute the bootstrap time function $t(a,m)$. Using the bootstrap rate obtained from the bootstrap dataset and the bootstrap time function, the second sequence of ordinary least square regression was carried out to obtain a solution for q_i, and q_∞. Figs. 15 and 16 shows the production forecast and uncertainty in the forecast for the 48-month hindcast.

3.2.4. Case 4: modified bootstrap with Duong's decline curve model

For the application of the modified bootstrap method with the Duong's model (MBM- Duong), we use the 48-month hindcast to generate multiple bootstrap samples. We computed the cumulative value, G_P, of the hindcast for the 48-month hindcast and then applied sequential linear regression and nonlinear regression to the hindcast dataset to obtain the Duong's model parameters. The residuals between the fitted data and actual production data were computed. The autocorrelation function and confidence limits were used to determine the block size. We then grouped the residuals into blocks of this size. We generated bootstrap datasets by adding the bootstrap samples of residuals to the fitted values of the regressed dataset. The parameters a, m, q_i, and q_∞ in Duong's model were obtained by applying two stages of sequential OLS regression to the bootstrap datasets.

Using parameters of the Duong's decline curve model obtained, future production was then forecasted, and probabilistic production estimates were calculated. Figs. 17 and 18 shows the production forecast and uncertainty in the forecast for the 48-month hindcast using MBM-Duong. We observe that the 48 month-

hindcast produced forecasts that mostly bracket the actual cumulative production. Also, the actual cumulative production uniformly falls within the P90 - P10 range, with the P50 value lying very close to the actual production value.

3.2.5. Case 5: conventional bootstrap with stretched exponential model

We obtained 100 bootstrap samples using the conventional bootstrap methodology and fit the SEDP model to obtain 100 values of the parameters τ, n, and $\hat{q}_i$ using nonlinear regression. Fig. 19 shows the production forecast and uncertainty for 48 months of pro-duction hindcast. The production forecast plot at 48 months of production hindcast often does not bracket the actual production. Fig. 20 gives the cumulative production plot at 48 months of production hindcast, using the conventional bootstrap with the SEPD model (CBM-SEPD). Actual reserves uniformly fall within the P90 - P10 range with the P50 value lying very close to the actual cumulative production value.

3.2.6. Case 6: modified bootstrap with stretched exponential model

Using 48 months of hindcast production data, we fit the SEPD model with nonlinear regression. We then computed the residuals and used the autocorrelation function to deter-mine the block size, with which we grouped the residuals into blocks as described previously. We obtained 100 new bootstrap datasets by adding the block bootstrap residuals to the fitted production data. Parameters τ, n, and $\hat{q}_i$ in the SEPD model were subsequently estimated from the bootstrap data. Future production was then forecasted, and probabilistic reserves estimates were determined. The production forecast and uncertainty in forecasts for 48 months of production hindcast is shown in Fig. 21. The production forecast plot mostly brackets the actual production. Fig. 22 gives the cumulative production plot at 48 months of production hindcast. Actual cumulative production uniformly falls within the P90 - P10 range, with the P50 value lying very close to the actual cumulative production

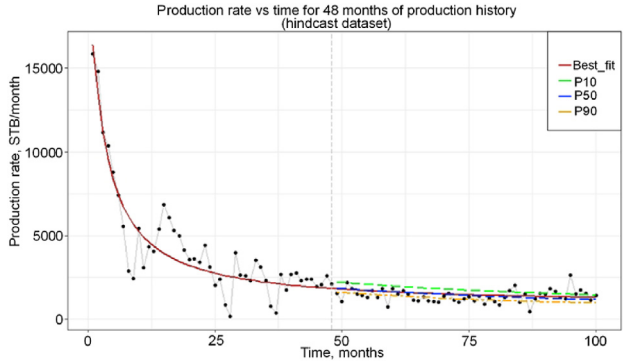

Fig. 17. The production forecast for 48 months of production data using Modified Bootstrap with Duong's model.

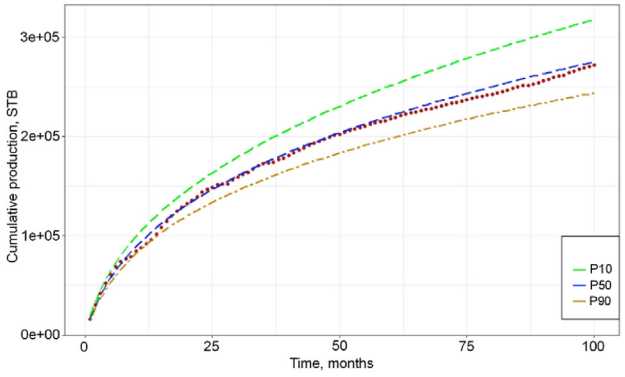

Fig. 18. Cumulative Production plot for 48 months of production data using Modified Bootstrap with Duong's model ("red" dotted line is best fit line).

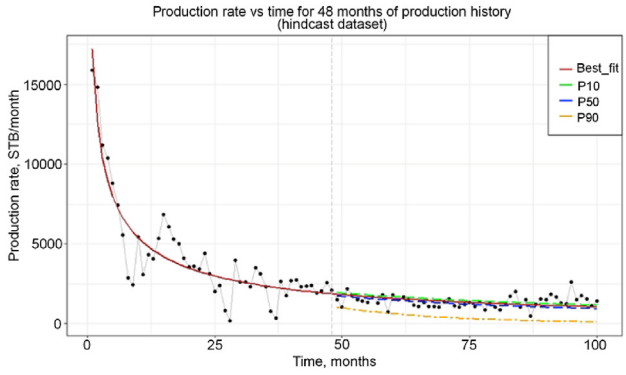

Fig. 19. The production forecast for 48 months of production data using Conventional Bootstrap with SEPD model.

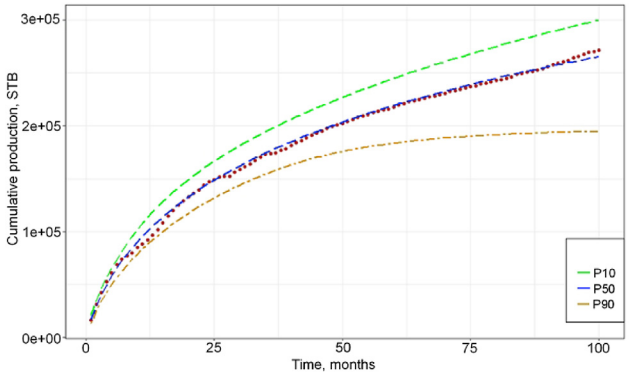

Fig. 20. Cumulative Production plot for 48 months of production data using Conventional Bootstrap with SEPD model ("red" dotted line is best fit line).

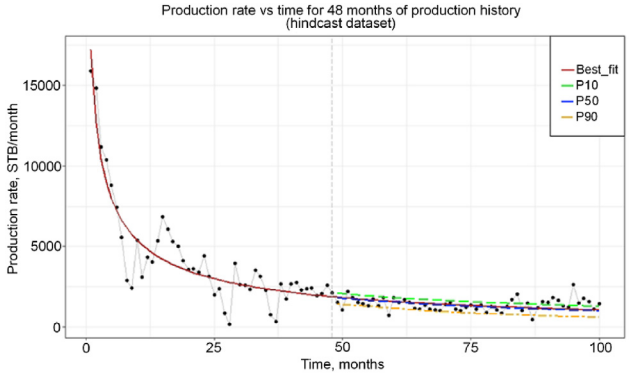

Fig. 21. The production forecast for 48 months of production data using Modified Bootstrap with the SEPD model.

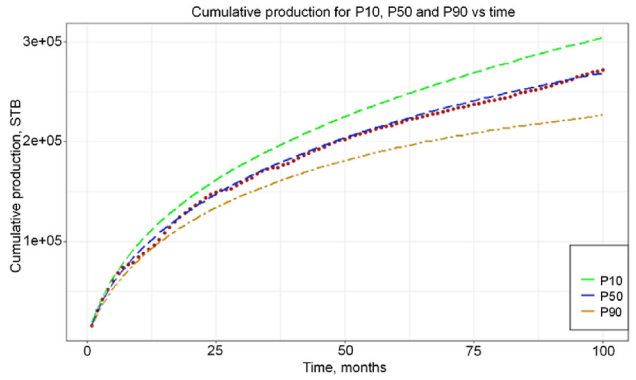

Fig. 22. Cumulative Production plot for 48 months of production data using Modified Bootstrap with the SEPD model ("red" dotted line is best fit line).

value.

Table 4 displays the average computation time, in seconds, of the different methodologies on a sample well. We found that the computational time is between 10 and 16 s per well on a standard engineering computer for a 48-month hindcast.

3.3. Application of the methodology to a set of wells from the Permian Basin

Figs. 23–26 consistently suggest that CBM-Arps, MBM-Arps, MBM-SEPD and to a lesser extent, MBM-Duong provide the best matches with actual data. We think the Duong model performed poorly from a prediction point of view for this dataset because we did not select data from the fracture-dominated flow regime only and the Duong model was developed mainly for wells still in the fracture-dominated flow regime.

We formalize the interpretation of these plots in Table 5, which reports the results of two-sided two-sample t-tests conducted between every pair of the six models. The variable tested is absolute error and the tests involve all wells in the Permian Basin. Significance at the 0.05 level (with a Bonferroni adjustment for the 45 tests performed) is indicated by a single asterisk for 12 months of hindcast, two asterisks for 36 months, and three asterisks for 60 months. The table is symmetric.

Figs. 23–26 and Table 5 show that, with respect to absolute error, there's little reason to prefer any one of CBM-Arps, MBM-Arps, and MBM-SEPD over the other two. These three model-algorithm combinations also consistently result in lower forecast errors. This group can be expanded to include MBM-Duong for hindcast lengths greater than 24 months.

Table 5 reports significant differences in coverage rate between some pairs of models in the Permian Basin. In our analysis of the coverage rate results, we focus on the three model-algorithm combinations we identified earlier as producing the lowest forecast errors, namely CBM-Arps, MBM-Arps, and MBM-SEPD. From Table 5, we observe that the CBM-Arps combination has statistically different coverage rates with the MBM-Duong and MBM-SEPD only at a 12-month hindcast and does not have statistically significant differences from the other model-algorithm combinations from the coverage rate point of view. We discourage the use of the Duong model at lower hindcast fractions because it results in excessive forecast errors, and we have previously identified the MBM-SEPD model as one of the best models from a forecast error viewpoint. Using similar reasoning for the MBM-Arps and MBM-SEPD

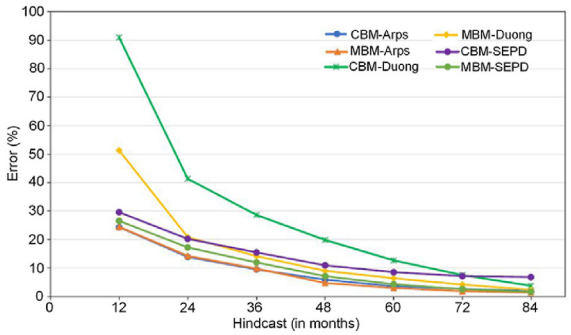

Fig. 23. Average Absolute Error plot for the forecast in Central Basin Platform.

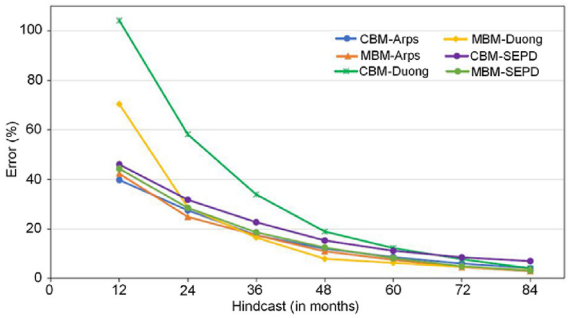

Fig. 24. Average Absolute Error plot for the forecast in Delaware Basin.

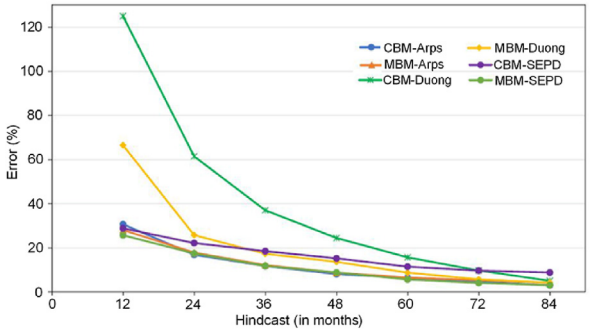

Fig. 25. Average Absolute Error plot for the forecast in Midland Basin.

Table 4
Computation time of each methodology with a bootstrap sample size of 100.

Methodology	CBM-Arps	MBM-Arps	CBM-Duong	MBM-Duong	CBM-SEPD	MBM-SEPD
Computation Time (in secs)	10.49	15.47	14.75	14.63	13.07	11.98

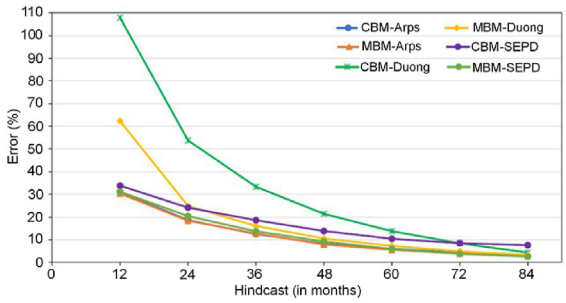

Fig. 26. Overall Average Absolute Error plot for the forecast in the Permian Basin.

combinations, we find that all the other model-algorithm combinations do not consistently offer superior coverage rate performance. As such, we conclude that the CBM-Arps, MBM-Arps, and MBM-SEPD model-algorithm combinations still remain the best models using both the forecast error and coverage rate as the evaluation metrics.

In view of the formal statistical tests above, Tables 6–9 summarize the best probabilistic models according jointly to the coverage rate and the average forecast error. In the Central Basin Platform, largely owing to coverage rates, the best probabilistic model is usually the CBM-SEPD combination, especially when one-quarter to one-half of the production history is used for hindcasting (Table 6). It should be noted however that other models (CBM-Arps, MBM-Arps and MBM-SEPD) perform better based on the forecast error. However, because the coverage rate reflects the ability of the probabilistic model to quantify uncertainty reliably, we have chosen the CBM-SEPD model as the best for the Central Basin Platform. Based on similar reasoning, we have chosen the MBM-Arps model as the best model for the wells in the Delaware Basin (Table 7) and either the CBM-Arps or the CBM-SEPD model as the best in the Midland Basin (Table 8). The best probabilistic model for the overall Permian Basin is the CBM-Arps when early time data is used as hindcast, CBM-SEPD for when one-quarter to one-half of the data is used as hindcast and MBM-SEPD for when greater than three-quarters of the production history is used as hindcast (Table 9). Table 10 shows the overall average absolute error in the Permian Basin.

We observe that both the rigorous formalized approach and the less rigorous approach based on the summary statistics result in

Table 5
Results of two-sided two-sample t-tests on absolute error (asterisks) and two-sample z-tests of proportions on coverage rate (daggers) between pairs of models for the Permian Basin. *† denote significance at 0.05 level for hindcast length 12 months; **†† 36 months; ***††† 60 months.

	CBM-Arps	MBM-Arps	CBM-Duong	MBM-Duong	CBM-SEPD	MBM-SEPD
CBM-Arps	–		* ** ***	* †	**	†
MBM-Arps		–	* † ** †† *** †††	* †	** †† ***	
CBM-Duong	* ** ***	* † ** †† *** †††	–	* † ** ***	* † ** ***	* † ** †† *** †††
MBM-Duong	* †	* †	* † ** ***	–	* †	*
CBM-SEPD	**	** †† ***	* † ** ***	* †	–	** †† ***
MBM-SEPD	†		* † ** †† *** †††	*	** †† ***	–

Table 6
Best probabilistic models based on coverage rate and forecast error for 42 wells in the Central Basin Platform (ideal coverage rate is 80%).

Months of production history used	Best Probabilistic model(s)	Forecast error (%)	Coverage Rate (%)
12	CBM-SEPD	30	55
24	CBM-SEPD	20	69
48	CBM-SEPD	11	79
72	MBM-SEPD	<5	81

Table 7
Best probabilistic models based on coverage rate and forecast error for 35 wells in the Delaware Basin (ideal coverage rate is 80%).

Approximate fraction of production history used	Best Probabilistic model(s)	Forecast error (%)	Coverage Rate (%)
12	MBM-Arps	42	41
24	MBM-Arps	25	37
48	MBM-Duong	8	74
72	MBM-SEPD	5	80

Table 8
Best probabilistic models based on coverage rate and forecast error for 49 wells in the Midland Basin (ideal coverage rate is 80%).

Approximate fraction of production history used	Best Probabilistic model(s)	Forecast error (%)	Coverage Rate (%)
12	CBM-Arps	31	70
24	CBM-SEPD	22	65
48	CBM-Arps	8	80
72	MBM-SEPD	<5	88

Table 9
Best probabilistic models based on coverage rate and forecast error in the overall Permian Basin (ideal coverage rate is 80%).

Approximate fraction of production history used	Best Probabilistic model(s)	Forecast error (%)	Coverage Rate (%)
12	CBM-Arps	31	64
24	CBM-SEPD	24	58
48	CBM-SEPD	14	75
72	MBM-SEPD	4	83

Table 10
Overall average absolute error in Permian basin.

Hindcast (in months)	CBM-Arps	MBM-Arps	CBM-Duong	MBM-Duong	CBM-SEPD	MBM-SEPD
12	31.06	30.37	107.93	62.33	33.86	31.17
24	18.69	18.37	53.81	24.92	24.18	20.43
36	12.44	12.78	33.37	16.07	18.65	13.74
48	8.29	7.96	21.39	10.53	13.82	9.26
60	5.99	5.55	13.75	7.29	10.42	5.92
72	4.38	3.93	8.46	4.91	8.50	3.78
84	2.92	2.89	4.35	3.35	7.64	2.60

broad agreement as it relates the model-algorithm combinations that best match the production data. The less formalized approach only adds the CBM-SEPD combination to the mix of best models in some specific instances.

Lastly, we noticed that the use of the Duong model with limited hindcast sizes (less than one-eighth of the available production history) resulted in large underestimations of cumulative production. As such, we will recommend that engineers not use the Duong model for probabilistic analysis when only limited production data history is available.

4. Limitations of work

This work is based solely on the analysis of production data. We understand that engineers working in the Permian Basin might have access to other data/factors related to the completion design, parent-child well interaction and formation information that might have some bearing on our conclusions. We also agree that the aforementioned factors might significantly affect well performance and the generalization of results from this study. However, this study is not concerned primarily with well performance or even necessarily the "best" model that will fit the data in a deterministic sense. It is primarily about computing the uncertainty associated with well performance and as such, we hope that the conclusions reached here can serve as base-level guidance for engineers trying to quantify the uncertainty associated with production data in the Permian Basin. Another limitation of our work is that we did not use hybrid DCA models. We recommend future researchers incorporate the use of hybrid models in uncertainty quantification especially as models that can efficiently describe the transition flow periods for the other commonly used DCA models become available.

5. Conclusions and recommendations

Based on a statistically rigorous analysis, the CBM-Arps, MBM-Arps, and MBM-SEPD combinations produce P50 forecasts that best match cumulative production regardless of the sub-basin and amount of production hindcast used. Also, the CBM-Arps, MBM Arps, and MBM-SEPD algorithm combinations produced cumulative P50 predictions that are approximately 20% of the true cumulative production value using only a 24-month hindcast (except for the Delaware Basin).

Based on the coverage rate and the forecast error plots (with the coverage rate being more significant in our choice of the best probabilistic models) and using up to one-half of the available production history for a group of sample wells from the Permian Basin, we have the following findings: (1) The CBM-SEPD combination is the best probabilistic model for the Central Basin Platform. (2) The MBM-Arps combination is the best probabilistic model for the Delaware Basin. (3) The CBM-Arps is the best probabilistic model for the Midland Basin. (4) The best probabilistic model for the overall Permian Basin is the CBM-Arps when early time data is used as hindcast and CBM-SEPD for when one-quarter to one-half of the data is used as hindcast. When three-quarters or more of the available production history is used for analysis, the MBM-SEPD probabilistic model is the best combination in terms of both coverage rate and forecast error. As expected, with increasing hindcast duration, the coverage rate increased, and the forecast error decreased for all the algorithm combinations. Also, the uncertainty bandwidth decreased with increasing production history. Consequently, the P90 - P10 intervals become narrower with increasing production history in all six methodologies.

Finally, it is important to note that the MBM algorithm did not decisively outperform the CBM algorithm across basins, hindcasts

lengths, and DCA model-pairings. Although it did evince modestly superior performance in specific instances, we find enough exceptions to conclude that the modifications to CBM described in subsection 2.3.5 do not sufficiently account for temporal autocorrelation in these data and with these DCA models. We regard the development of an effective modified bootstrap methodology to be a question worth future additional investigation.

Declaration of competing interest

On behalf of all authors, the corresponding author states that there is no conflict of interest.

Appendix A. Linearizing the Arps' Decline Curve Equation

The Arps' decline-curve equations for hyperbolic decline is given by:

$$q(t) = \frac{q_i}{(1 + D_i b t)^{\frac{1}{b}}} \tag{A.1}$$

where:

q is the current production rate, q_i is the production rate at time zero, b is hyperbolic decline constant, t is the time since the start of production, D_i is initial decline rate.

We can linearize the hyperbolic decline curve equation by taking the logarithm of both sides and simplifying

$$q(t) = \frac{q_i}{(1 + D_i b t)^{\frac{1}{b}}}$$

$$q(t) = q_i (1 + D_i b t)^{-\frac{1}{b}}$$

$$\log q = \log q_i + \log (1 + b D_i t)^{-\frac{1}{b}}$$

$$\log q = \log q_i - \frac{1}{b} \log(1 + b D_i t)$$

Applying a second-order Taylor series ex: $\log(1+x) \approx x - \frac{x^2}{2}$ pansion

$$\log q \approx \log q_i - \frac{1}{b}\left(b D_i t - \frac{(b D_i t)^2}{2}\right)$$

$$\log q \approx \log q_i - D_i t + \frac{b D_i^2 t^2}{2}$$

This can be expressed as a second-order linear regression model

$$\therefore \log q = \widehat{\beta_0} + \widehat{\beta_1} t + \widehat{\beta_2} t^2 \tag{A.2}$$

where $\widehat{\beta_0} = \log q_i, \widehat{\beta_1} = -D_i, \widehat{\beta_2} = \frac{b D_i^2}{2}$

From Equation (A.2), the decline curve parameter estimates $\widehat{q_1}$, $\widehat{b}$, and $\widehat{D_i}$ can be obtained

$$\widehat{q_1} = \exp\widehat{\beta_0}, \widehat{D_i} = -\widehat{\beta_1}, \widehat{b} = \frac{2\widehat{\beta_2}}{\widehat{\beta_1}^2} \tag{A.3}$$

Appendix B. Sequential Linear Regression Analysis to obtain Duong's Decline Curve Parameters

From Duong's log-log plots for rate over cumulative production versus time, we have that:

$$\frac{q}{G_p} = a t^{-m} \tag{B.1}$$

where: q is production rate, G_p is cumulative production rate, a is intercept, m is the slope of the log-log plot.

We can take the logarithm of both sides and simplify the equation above to obtain a linear equation:

$$\log\left(\frac{q}{G_p}\right) = -m \log(t) + \log a \tag{B.2}$$

This can be expressed in terms of β coefficients as $\widehat{y_i} = \widehat{\beta_0} + \widehat{\beta_1} x_1$ with *intercept* $\widehat{\beta_0}$ and *slope* $\widehat{\beta_1}$ hence $\widehat{y_i} = \log\left(\frac{q}{G_p}\right)$, $\widehat{\beta_0} = \log a, \widehat{\beta_1} = -m,$ and $x_1 = \log(t)$. The parameter estimates a and m can be obtained as:

$$\widehat{a} = \exp\widehat{\beta_0}, \widehat{m} = -\widehat{\beta_1} \tag{B.3}$$

The values of a and m is then used to obtain an expression for the time function $t(a,m)$ defined as: $t(a,m) = t^{-m} \exp\left[\frac{a}{1-m}(t^{1-m} - 1)\right]$. Subsequently, a second linear regression is carried out to obtain estimates for q_i and q_∞ using the Duong's model equation:

$$q = q_i t(a,m) + q_\infty \tag{B.4}$$

By using two stages of sequential ordinary least square regression, all four parameters

(a, m, q_i, q_∞) in the Duong's model can be obtained

Appendix C. Fitting algorithms used in this research

The table below highlights the fitting algorithms used in this work. Several selected solvers for different curves are also listed.

Table C.3
Selected Solvers for different curves

Model	Solver in R	Parameters
CBM-Arps	nls regression	$\widehat{q_i}, \widehat{b}$ *and* $\widehat{D_i}$
CBM-Duong	ols regression	a, m, q_i, q_∞
CBM-SEPD	nls regression	τ, n, and $\widehat{q_i}$
MBM-Arps	nls regression	$\widehat{q_i}, \widehat{b}$ *and* $\widehat{D_i}$
MBM-Duong	ols regression	a, m, q_i, q_∞
MBM-SEPD	nls regression	τ, n, and $\widehat{q_i}$

The ordinary least squares (ols) regression solver uses the *lm* function for performing regression analysis in **R**. The nonlinear least squares (nls) regression solver uses the *nls* function to find parameter values for non-linear functions.

References

Arps, J.J., 1945. Analysis of decline curves. Transactions of the AIME 160, 228–247. https://doi.org/10.2118/945228-G.

Can, B., Kabir, C.S., 2011. Probabilistic performance forecasting for unconventional reservoirs with stretched exponential model. In: North American Unconventional Gas Conference and Exhibition. https://doi.org/10.2118/143666-MS.

Cheng, Y., Wang, Y., McVay, D.A., Lee, W.J., 2010. Practical application of a probabilistic approach to estimate reserves using production decline data. SPE Econ. Manag. 2, 19–31. https://doi.org/10.2118/95974-PA.

Duong, A.N., 2011. Rate-decline analysis for fracture-dominated shale reservoirs. SPE Reservoir Eval. Eng. 14, 377–387. https://doi.org/10.2118/137748-PA.

Gong, X., Gonzalez, R., McVay, D.A., Jeffrey, D.H., 2014. Bayesian probabilistic decline-curve analysis reliably quantifies uncertainty in shale-well-production forecasts. SPE J. 19, 1047–1057. https://doi.org/10.2118/147588-PA.

Gorditsa, M., Bryan, E., Moridis, G.J., Blasingame, T.A., 2020. Mechanistic model validation of decline curve analysis for unconventional reservoirs. In: SPE Annual Technical Conference and Exhibition, Virtual. https://doi.org/10.2118/201658-MS.

Jochen, V.A., Spivey, J.P., 1996. Probabilistic reserves estimation using decline curve analysis with the bootstrap method. In: SPE Annual Technical Conference and Exhibition. https://doi.org/10.2118/36633-MS. Denver, Colorado, USA.

Khanal, A., Khoshghadam, M., Makinde, I., Lee, W.J., 2015. Modeling production decline in liquid rich shale (LRS) gas condensate reservoirs. In: SPE/CSUR Unconventional Resources Conference. Canada, Calgary, Alberta. https://doi.org/10.2118/175913-MS.

Klie, H., 2015. Physics-based and data-driven surrogates for production forecasting. In: SPE Reservoir Simulation Symposium. Houston, Texas, USA. https://onepetro.org/spersc/proceedings-abstract/15RSS/2-15RSS/D021S007R005/183443.

Kong, B., Chen, S., Chen, Z., Zhou, Q., 2020. Bayesian probabilistic dual-flow-regime decline curve analysis for complex production profile evaluation. J. Petrol. Sci. Eng. 195. https://doi.org/10.1016/j.petrol.2020.107623.

Korde, A., Goddard, Scott D., Awoleke, Obadare O., 2021. Probabilistic decline curve analysis in the Permian Basin using Bayesian and approximate Bayesian inference. SPE Reservoir Eval. Eng. 24, 536–551. https://doi.org/10.2118/204477-PA.

Li, Y., Han, Y., 2017. Decline curve analysis for production forecasting based on machine learning. In: SPE Symposium: Production Enhancement and Cost Optimisation. Kuala Lumpur, Malaysia. https://doi.org/10.2118/189205-MS.

Liu, H., Zhang, J., Liang, F., Temizel, C., Basri, M.A., Mesdour, R., 2021. Incorporation of physics into machine learning for production prediction from unconventional reservoirs: a Brief review of the gray-Box approach. SPE Reservoir Eval. Eng. 24, 847–858. https://doi.org/10.2118/205520-PA.

Makinde, I., Lee, John W., 2016a. Forecasting production of shale volatile oil reservoirs using simple models. In: SPE/IAEE Hydrocarbon Economics and Evaluation Symposium. https://doi.org/10.2118/179964-MS. Houston, Texas, USA.

Makinde, I., Lee, John W., 2016b. Production forecasting in shale volatile oil reservoirs using reservoir simulation, empirical and analytical methods. In: SPE/AAPG/SEG Unconventional Resources Technology Conference. https://doi.org/10.15530/URTEC-2016-2429922. San Antonio, Texas, USA.

Ogunyomi, B.A., Dong, S., La, N., Lake, L.W., Kabir, C.S., 2014. A new approach to modeling production decline in unconventional formations. In: SPE Annual Technical Conference and Exhibition. The Netherlands, Amsterdam. https://doi.org/10.2118/170899-MS.

Paryani, M., Awoleke, O.O., Ahmadi, M., Hanks, C., Barry, R., 2017. Approximate Bayesian computation for probabilistic decline curve analysis in unconventional reservoirs. SPE Reservoir Eval. Eng. 20, 478–485. https://doi.org/10.2118/183650-PA.

Purvis, D.C., Kuzma, H., 2016. Evolution of uncertainty methods in decline curve analysis. In: SPE/IAEE Hydrocarbon Economics and Evaluation Symposium. https://doi.org/10.2118/179980-MS. Houston, Texas, USA.

R Core Team, 2022. R: A Language and Environment for Statistical Computing. R Foundation for Statistical Computing, Vienna, Austria. URL. https://www.R-project.org/.

U.S. EIA, 2020. Permian Basin - Part 1: Wolfcamp, Bone Spring, Delaware Shale Plays of the Delaware Basin. Technical Report. https://www.eia.gov/maps/pdf/Permian-pl_Wolfcamp-Bonespring-Delaware.pdf.

Valko, Peter P., Lee, John W., 2010. A better way to forecast production from unconventional gas wells. In: SPE Annual Technical Conference and Exhibition. Italy, Florence. https://doi.org/10.2118/134231-MS.

Ward, R.F., Kendall, C.G., Harris, P.M., 1986. Upper permian (guadalupian) facies and their association with hydrocarbons–permian basin, west Texas, and New Mexico. Am. Assoc. Petrol. Geol. Bull. 70 (12), 1671–1674.